nature geoscience

LETTERS

PUBLISHED ONLINE: 12 OCTOBER 2014 | DOI: 10.1038/NGEO2252

Evidence for basaltic volcanism on the Moon within the past 100 million years

S. E. Braden[1]*, J. D. Stopar[1], M. S. Robinson[1], S. J. Lawrence[1], C. H. van der Bogert[2] and H. Hiesinger[2]

The bulk of basaltic magmatism on the Moon occurred from 3.9 to 3.1 billion years ago on the ancient lunar mare plains[1]. There is evidence for basaltic volcanism as recently as 2.9 billion years ago from crystallization ages[2] and a billion years ago from stratigraphy[3,4]. An enigmatic surface formation named Ina (18.65° N, 5.30° E) may represent much younger mare volcanism, but age estimates are poorly constrained[5–8]. Here we investigate 70 small topographic anomalies, termed irregular mare patches (100–5,000 m maximum dimension), on the lunar nearside with irregular morphologies and textures similar to Ina, using Lunar Reconnaissance Orbiter narrow angle camera images[9], digital terrain models and wide angle camera colour ratios. The irregular mare patches exhibit sharp, metre-scale morphology with relatively few superposed impact craters larger than ten metres in diameter. Crater distributions from the three largest irregular mare patches imply ages younger than 100 million years, based on chronology models of the lunar surface[10,11]. The morphology of the features is also consistent with small basaltic eruptions that occurred significantly after the established cessation of lunar mare basaltic volcanism. Such late-stage eruptions suggest a long decline of lunar volcanism and constrain models of the Moon's thermal evolution.

Irregular mare patches (IMPs), including the formation known as Ina (18.65° N, 5.30° E; refs 5–8,12), are characterized by their distinct irregular morphology and texture and relatively small size compared to the maria. In this paper, we document 70 IMPs, with maximum dimensions from 100 to 5,000 m and an average maximum dimension of 485 m ($n = 70$, s.d. = 829 m). This survey significantly expands the known IMP inventory, 16 of which were noted by previous authors (Fig. 1, Supplementary Table 1 and Supplementary Figs 1 and 2). Ina is the only extensively studied IMP (Fig. 2i and Supplementary Fig. 3; refs 5–8,12). Beginning with Apollo era investigations, Ina was interpreted as a collapsed caldera at the summit of a low-shield volcano[6,7]. Interpretation of impact crater densities within and around Ina indicate that it is younger than the surrounding mare basalt unit in Lacus Felicitatis[6,7], and give a suggested maximum age for Ina of 10 Myr (ref. 8).

IMPs comprise two morphologically distinct deposits (Fig. 2; refs 7,12). The topographically uneven deposit has a visibly rough surface texture (relative to the smooth deposit) and a range of block densities. In contrast, the smooth deposit has a relatively uniform texture and almost no blocks. Both deposits are characterized by a paucity of superposed impact craters with diameters $D \geq 10$ m compared to mature mare. An abrupt change in slope marks the contacts between the two deposits, and the smooth deposits exhibit lobate margins and steep slopes at the contact. Stratigraphic relationships at all IMPs indicate that the smooth deposits generally superpose—and are higher in elevation than—the uneven deposits.

Crater size-frequency distributions (CSFDs; refs 10,11) of superposed craters with $D \geq 10$ m yield model ages for the smooth deposits of individual IMPs (Fig. 3), but the uneven deposits have too few craters to provide statistically significant CSFDs (Methods section); however, their inferred stratigraphic position below the smooth deposits suggests an older age. Model ages are 58 ± 4 Myr for the Cauchy-5 IMP (smooth deposit area = 1.3 km^2), 33 ± 2 Myr for Ina (smooth deposit area = 1.7 km^2) and 18 ± 1 Myr for the Sosigenes IMP (smooth deposit area = 4.5 km^2) (Supplementary Figs 4 and 5). The cumulative numbers of craters (N_{cum}) with $D \geq 10$ m per unit area (km^2) were compared to other young lunar surfaces to provide another measure of overall crater density. The smooth deposits of the Cauchy-5, Ina and Sosigenes IMPs have N_{cum} ($D \geq 10$ m) per unit area of 202, 137 and 64, respectively. The $N_{cum}(D \geq 10\,\text{m})$ for each of the three IMPs is similar to or less than the reported $N_{cum}(D \geq 10\,\text{m})$ from CSFDs of North Ray ejecta ($\sim 47 \pm 4$ Myr and $N_{cum}[D \geq 10\,\text{m}] = 180$) (ref. 13), and thus implies

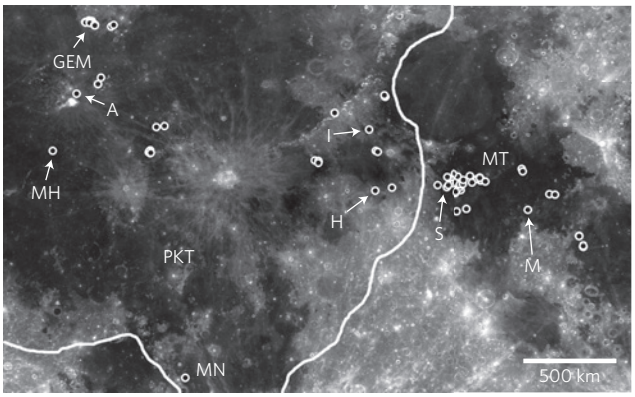

Figure 1 | Distribution of IMPs on the nearside. Each dot represents either a single >100 m diameter IMP, or a cluster of smaller IMPs. The white line defines the approximate boundary of the Procellarum KREEP Terrane (PKT), which is characterized by thorium concentrations generally exceeding 3.5 ppm (ref. 20). Mare Tranquillitatis (MT) is not considered part of the PKT. The map extends from −28.0° N to 40.6° N latitude and −58.0° E to 50.3° E longitude. The basemap is the LROC WAC 643 nm normalized reflectance mosaic. Abbreviations: Aristarchus (A), Gruithuisen E-M region (GEM), Marius Hills (MH), Mare Nubium (MN), Ina (I), Hyginus (H), Sosigenes (S), Maskelyne (M). Image: NASA/GSFC/Arizona State University.

[1]School of Earth and Space Exploration, Arizona State University, 1100 S. Cady Mall, Interdisciplinary A, Tempe, Arizona 85287-3603, USA, [2]Institut für Planetologie, Westfälische Wilhelms-Universität Münster, Wilhelm-Klemm-Str. 10, 48149 Münster, Germany, *e-mail: sebraden@asu.edu

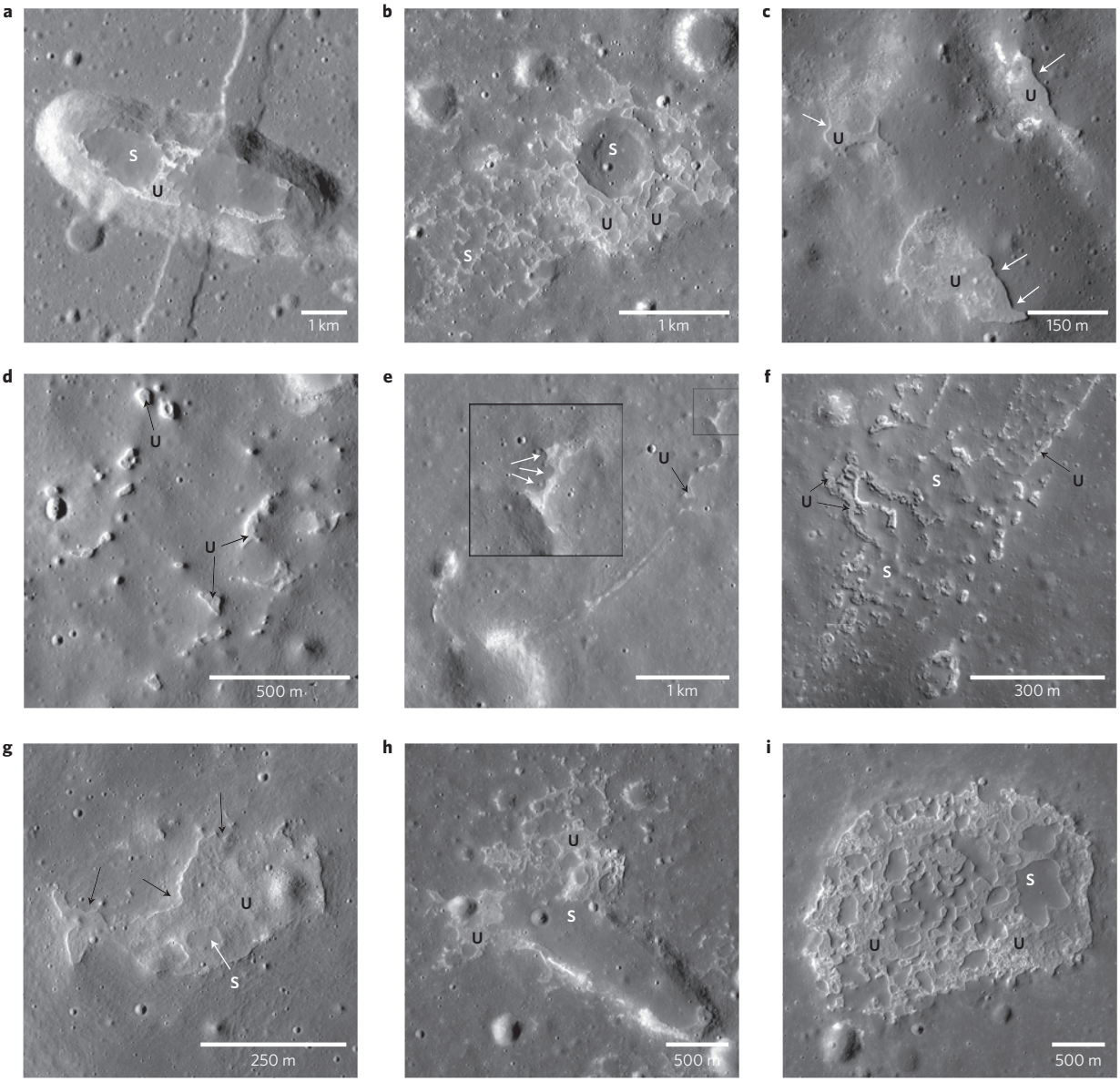

Figure 2 | Examples of IMPs. Locations listed in Supplementary Table 1. Examples of smooth and uneven deposits marked with 'S' and 'U'. **a**, Topographic depression containing the Sosigenes IMP (LROC NACs M192832116, M192824968). **b**, Maskelyne IMP. Circular topographic high right of centre (M1123370138R). **c**, Manilus-1 IMP. Sharp, lobate contacts (white arrows) where the smooth deposits superposed the uneven deposit (M113914588R). **d**, IMP inside Hyginus crater (M1108239463). **e**, Carrel-1 IMP. Narrow, discontinuous sections of uneven deposits may be a vent rim remnant. The inset highlights three lobate contacts (white arrows) (M1096329585). **f**, IMP north of Aristarchus crater (M168509312R). **g**, Maclear-1 IMP. Black arrows point to lobate margins (M177494593R). **h**, Cauchy-5 IMP. Superposed on a 6 km diameter volcano (M1108025067). **i**, Ina exhibits numerous connected and isolated smooth deposits (M113921307). Images: NASA/GSFC/Arizona State University.

a young age for the IMPs, roughly similar to or younger than North Ray crater ($\leq$50 Myr; ref. 13).

The absence of clear equilibrium diameters for the Cauchy-5, Ina and Sosigenes IMPs suggests they are younger than the Tycho ejecta, which has the lowest measured equilibrium diameter reported for craters with well-constrained CSFD age estimates. The CSFD of Tycho ejecta (area = 1.65 km^2) gives a model age of ~85 +15/−18 Myr with the equilibrium population at $D \leq 12$ m (ref. 13). For comparison, the CSFD of the older Copernicus ejecta blanket (area = 121 km^2) produces a model age of ~797 Myr and is in equilibrium at $D \leq 70$ m (ref. 13). Equilibrium diameter is the diameter at which craters are destroyed at the same rate they are produced and is identified as a break in the slope of the CSFD for a unit; CSFDs of younger surfaces have smaller equilibrium crater diameters[14]. On the basis of a comparison of the three IMPs and Tycho ejecta we propose 100 Myr as a conservative upper age constraint for the IMPs with CSFDs presented here. Furthermore, equilibrium diameters from mare basalt surfaces are large enough (~150–300 m) such that if IMPs were of similar age to mare basalts, some IMPs would not be visible at present. For example, the CSFD for Mare Tranquillitatis near the Sosigenes IMP exhibits equilibrium at $D \leq 290$ m (model age ~3.5 +0.09/−0.05 Ga; ref. 4).

In addition, we note that an IMP (~800 m by 400 m; 25.044° N, 313.233° E) occurs superposed on the continuous ejecta blanket of Aristarchus crater (42 km diameter), 25 km from the rim (Fig. 2f and Supplementary Fig. 6). At this distance, the emplacement of the ejecta would have destroyed the morphologically sharp, metre-scale details of the Aristarchus IMP if it pre-dated Aristarchus

crater. Furthermore, the Clementine optical maturity parameter (OMAT; ref. 15) value (~0.34) of the Aristarchus IMP is distinct and immature relative to the surrounding crater ejecta (0.22–0.27). CSFDs derived for the entire proximal ejecta blanket of Aristarchus yield model ages of ~189 Myr for $D \geq 60$ m and ~150 Myr for $D \geq 200$ m (ref. 16). The location, superposition on the Aristarchus continuous ejecta, and OMAT values of this IMP are consistent with an age younger than the Aristarchus crater.

Narrow angle camera (NAC) digital terrain models (DTMs; Supplementary Table 2) enable quantitative assessment of IMP smooth deposit margin slopes and relief (total elevation difference) near the smooth/uneven deposit contacts for six IMPs (Supplementary Figs 7 and 8). Smooth deposits have average margin slopes as follows: 26° (range 14–39°) at Ina; 22° (range 13–30°) at Hyginus; 16° at Sosigenes and Maclear-1 (ranges 8–32° and 5–37°, respectively); 14° (range 9–24°) at Manilus-1; and 8°, the shallowest average slope, at Cauchy-5 (range 3–12°). The slopes are measured over a minimum of three pixels, which equates to a length of 6 m (for 2 m pixel^{-1} DTMs) or 15 m (for 5 m per pixel DTMs); steeper slopes may exist at smaller length scales below the detection limit of the DTMs. The measured average margin slopes are less than the angle of repose (30–35°), but the maximum slope sometimes exceeds 30°. Processes contributing to decreasing slopes on the lunar surface over time are steady erosion through meteorite bombardment, seismic shaking due to moonquakes, and downslope movement caused by gravity. Although slopes near the angle of repose, 30–35°, are consistent with a young (Copernican) age for the smooth deposits, slopes <30–35° do not rule out a young age, as materials can be initially emplaced with lower slopes. The average 8 m relief of the smooth deposits (average of 143 measurements, range 2 to 20 m) overlaps with previous estimates of mare basalt flow thicknesses, which range from <8 m (ref. 17) to 35 m (ref. 18); the average relief of the smooth deposits is consistent with their emplacement as basaltic lava flows.

IMPs have CSFDs and sharp, steep contacts that are distinct from nearby older mare basalts, but the contact with the surrounding mare material is often ambiguous or gradational (for example, Manilus-1, Carrel-1 and Maclear-1; Fig. 2). Within the larger IMPs (Ina, Maskelyne and Cauchy; Fig. 2), there are isolated areas of smooth deposits entirely surrounded by uneven deposits. Smaller IMPs do not always have isolated smooth deposits, but do have smooth deposits connected to the surrounding mare. The smooth deposits consistently have lobate margins and steep boundary slopes, and superpose the uneven deposits. Lobate margins at the contacts between smooth and uneven deposits in IMPs such as Ina, Cauchy-5 and Maskelayne are suggestive of volcanic materials flowing towards topographically lower areas. These IMPs are associated with volcanic vents, which suggests that at least some of the IMPs occur as a result of volcanic eruptions. Smooth deposits could represent lavas emplaced during terminal-stage eruptions, some of which flowed back into the vent area (see, for example, ref. 12). The stratigraphically lower uneven deposits may have formed as the eruptive vent collapsed, fragmenting pre-existing basalt within the vent (or perhaps disrupting a lava lake crust[7]). The upper deposits remained smooth because they formed after the terminal collapse event.

Multispectral data from the IMPs determined that they are consistent with mare materials. The wide angle camera (WAC) colour ratios (320/415 nm) of material within and immediately surrounding the five largest IMPs range from 0.75 to 0.85, which is within the distribution of ratio values for mare material (0.70–0.85; Supplementary Fig. 9 and Table 4). Previous multispectral investigations of Ina showed that the uneven deposits have a higher reflectance at blue wavelengths (460 nm) and a stronger ferrous absorption (1 μm band measured by 750/990 nm ratio) relative to the surrounding area and the smooth deposits[8,19]. The stronger

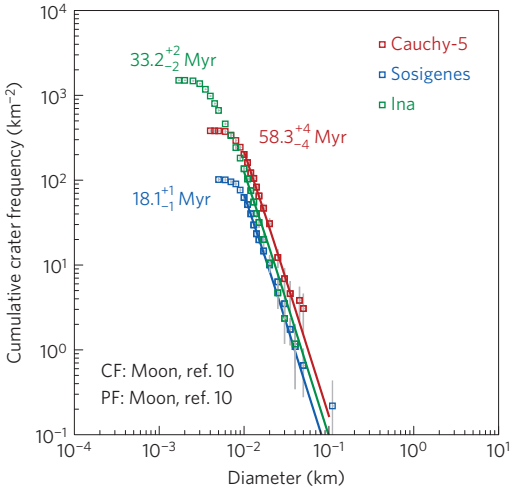

Figure 3 | CSFDs from IMPs. CSFDs derived from smooth deposits within the Cauchy-5 (red), Sosigenes (blue) and Ina (green) IMPs give a range of model ages, using the chronology functions (CF) and production functions (PF) of ref. 10 from 18–58 Myr. Statistical error bars[11] are shown in grey.

mafic absorptions of the uneven deposits at Ina, in addition to the higher 415/750 nm ratios, were considered consistent with the exposure of immature high-titanium basalts[8,19]. The uneven deposits are blockier than the smooth deposits, and the constant breakdown of blocks due to micrometeorite bombardment provides a less mature surface than the surroundings.

The known IMPs are widely distributed across the nearside maria, found from −46.8° E to 43.5° E longitude and −25.7° N to 38.2° N latitude (Fig. 1). Given the relative surface areas of nearside and farside maria (31% of the nearside and only 1% of the farside) and the observed nearside mare IMP population ($n = 70$), we expect to observe ~3 IMPs ≥100 m within the farside maria; however, none have been found. A thicker farside crust may restrict the rise of late-stage magma to the surface, or perhaps differences in the distribution of long-lived radiogenic heat sources in the mantle (probably required for young volcanic eruptions) caused the observed absence of farside IMPs. However, the distribution of IMPs is not restricted to areas with thorium enhancements (>3.5 ppm Th). About half of the IMPs are outside of the Procellarum KREEP Terrane (PKT) boundary (>~3.5 ppm Th by definition)[20] (Fig. 1), whereas ~30% of IMPs are found in locations with <3.5 ppm Th. About 70% of IMPs are found in two areas: the northwestern half of Mare Tranquillitatis and the region near impact craters Gruithuisen E and M (Fig. 1, Supplementary Table 1). The occurrence of IMPs across much of the nearside suggests recent volcanic activity, consistent with the proposed existence of an 'urKREEP' mantle layer enriched in incompatible, heat-producing elements[21].

The population of newly discovered IMPs is widely dispersed across the lunar nearside and provides further evidence for late Copernican period (<500 Myr) basaltic volcanism. The basaltic flows of the IMPs (smooth deposits) are significantly smaller in volume than the lunar maria, consistent with short-duration, late-stage eruptions. The existence of Ina[5] and other IMPs[8] provides evidence for a period of young basaltic volcanism more recent than the commonly accepted cessation of basaltic volcanism ~1–1.2 Ga ago (for example, refs 1–4). Young, small-volume extrusions of mare basalt imply a thermal history where mare volcanism did not end abruptly, but rather decreased gradually over time[3,22,23]. The existence and inferred late Copernican ages of the IMPs have implications for models of lunar thermal evolution (such as those in ref. 23), which must provide enough heat to account

for small-volume eruptions late into the Copernican period. Ina and other IMPs are excellent candidates for future exploration, including sample return missions. Sample return will be required for radiometric age dating to confirm the relatively young ages implied by remote sensing observations.

Methods

Data used in this study include Lunar Reconnaissance Orbiter Camera (LROC) NAC nadir-pointing images, LROC WAC and Clementine Ultraviolet/Visible (UVVIS) multispectral observations, Lunar Prospector gamma-ray spectrometer thorium maps at 0.5° per pixel, and DTMs derived from NAC stereo pairs. All of the raw and calibrated NAC and WAC image data are available through the NASA Planetary Data System (http://lroc.sese.asu.edu/data/).

LROC NAC image data were calibrated and projected using Integrated Software for Imagers and Spectrometers (ISIS). CSFDs were derived from NAC images of the following IMPs: Sosigenes (M192824968, incidence angle = 70°, scale = 1.2 m pixel^{-1}), Ina (M113921307, incidence angle = 58°, scale = 0.5 m pixel^{-1}) and Cauchy-5 (M1108039362, incidence angle = 63°, scale = 1.2 m pixel^{-1}). Craters on each mapped unit and the surrounding mare were digitized (diameter and centre location) using ArcGIS CraterTools[24] and CSFDs were plotted using CraterStats2 (ref. 11). The CraterStats2 model ages are based on the production function and chronology function of ref. 10 for lunar craters $0.01 < D < 100$ km. Absolute model ages were derived only for craters with $D \geq 10$ m, although the NAC pixel scale (0.5–1.5 m) allows the discrimination of smaller craters (see, for example, ref. 13). The numbers of impact craters found on each IMP deposit are documented in Supplementary Table 3.

Owing to the small area of each IMP and the small diameters of the impact craters within those areas, a few caveats should be considered when interpreting the model ages. First, CSFDs of craters $D < 1$ km may be contaminated by secondary craters[25]. All of the craters in CSFDs reported here are for craters $D < 1$ km, so all craters are within the dominant size regime of secondaries ($D < 1$ km). No obvious secondaries are visible on the subset of IMPs used for crater statistics, and so all craters were included in the CSFDs. Accidental inclusion of secondary craters would artificially increase absolute model ages, resulting in an overestimation of the absolute model ages of the IMPs. Thus, if undetected secondaries were included in our counts, the absolute model ages are maximum ages (that is, the true age of the IMPs would be younger). Second, the diameters of the craters are within the strength-scaling regime, such that target properties might affect the final crater diameters and, thus, the absolute model age calculations[26,27]. Discrepancies between crater diameters in contemporaneous geologic units could be 20%, based on empirical observations at Jackson crater[27], or even up to 50%, based on pi-scale modelling of final crater diameters on differing targets[28]. If the diameters of the CSFDs of the youngest and oldest IMPs are adjusted to assess the possible error introduced by target properties, the absolute model ages could shift as much as 85 Myr (Supplementary Fig. 10). Thus, regardless of the possible effect of target properties on the ages, the IMPs still yield late Copernican model ages.

The minimum area required to accurately date a surface depends on crater density, to provide a sufficient number of craters for good statistics. Small, young surfaces may be limited in extent and thus only contain a small sample of craters. Comparison of CSFDs measured at both WAC and NAC scales for both large and small count areas on impact ejecta units at Copernican craters indicate that small count areas (<0.5 km^2) are adequate for dating these units, yielding absolute model ages consistent with ages from Apollo samples[13]. For example, the individual count areas (0.41–0.84 km^2) at North Ray crater give ages ranging from 39 +7/−8 Myr to 61 +9/−11 Myr, with an average age of 46–47 ± 4 Myr (ref. 13). The age of North Ray crater, based on Apollo sample analysis, is well constrained at ∼50 Myr (ref. 29 and references therein). The similarity of both results lends support to the validity of applying CSFD measurements to the dating of young surfaces on the Moon using small-diameter craters and small areas[13,29].

Multispectral analyses using 950/750 nm (Clementine; indicative of the mafic band strength) and 320/415 nm (LROC WAC; indicative of the opaque content) band ratios were possible for five IMPs. The five IMPs Maskelyne, Ina, Cauchy-5, Sosigenes and Nubium were large enough (2,000–5,000 m) to be resolved in the WAC UV mosaic (∼400 m pixel^{-1}). The Clementine UVVIS global mosaic was sampled at 400 m pixel^{-1} with an equirectangular projection to match. The WAC images were calibrated and projected using ISIS and photometrically corrected with an empirical algorithm[30]. Each sample area was 15 × 15 pixels, and in the case of the IMPs the samples contain both smooth and uneven deposits, as well as material immediately external to the IMPs.

NAC DTMs were created with pixel scales four times that of the original NAC stereo observations. Elevation profiles from the DTMs are then used to measure slopes and relief. Each slope measurement included at least three pixels, which for the 2-m DTM products results in slope measurements over at least a 6 m length and for the 5-m DTM slope measurements are calculated over at least a 15 m length. Any slope changes below 6 or 15 m are not detectable by measurements made from the DTMs, including differences in surface roughness between the uneven and smooth material. The relief of the smooth deposits was measured using the elevation of the uneven material at the contact of the smooth and uneven deposits as a baseline. Then the elevation of the smooth material ∼200 m from the contact was recorded and the difference from the baseline was considered the relief of the smooth deposits.

Received 22 January 2014; accepted 20 August 2014; published online 12 October 2014

References

1. Basaltic Volcanism Study Project *Basaltic Volcanism on the Terrestrial Planets* 1286 (Pergamon, 1981).
2. Borg, L. E., Shearer, C. K., Asmerom, Y. & Papike, J. J. Prolonged KREEP magmatism on the Moon indicated by the youngest dated lunar igneous rock. *Nature* **432,** 209–211 (2004).
3. Schultz, P. H. & Spudis, P. D. Beginning and end of lunar mare volcanism. *Nature* **302,** 233–236 (1983).
4. Hiesinger, H., Head, J. W., Wolf, U., Jaumann, R. & Neukum, G. Ages and stratigraphy of lunar mare basalts: A synthesis. *GSA Special Papers* **477,** 1–51 (2011).
5. Whitaker, E. A. in *Apollo 15 Preliminary Science Report*, NASA SP-289, Ch. 25, 84–85 (NASA, 1972).
6. El-Baz, F. in *Apollo 17 Preliminary Science Report*, NASA SP-330, Ch. 30, 13–17 (NASA, 1973).
7. Strain, P. L. & El-Baz, F. The geology and morphology of Ina. *Proc. Lunar Sci. Conf.* **11,** 2437–2446 (1980).
8. Schultz, P. H., Staid, M. I. & Pieters, C. M. Lunar activity from recent gas release. *Nature* **444,** 184–186 (2006).
9. Robinson, M. S. *et al.* Lunar Reconnaissance Orbiter Camera (LROC) instrument overview. *Space Sci. Rev.* **150,** 81–124 (2010).
10. Neukum, G., Ivanov, B. A. & Hartmann, W. K. Cratering records in the inner solar system in relation to the lunar reference system. *Space Sci. Rev.* **96,** 55–86 (2001).
11. Michael, G. G. & Neukum, G. Planetary surface dating from crater size-frequency distribution measurements: Partial resurfacing events and statistical age uncertainty. *Earth Planet. Sci. Lett.* **294,** 223–229 (2010).
12. Garry, W. B. *et al.* The origin of Ina: Evidence for inflated lava flows on the Moon. *J. Geophys. Res.* **117,** E00H31 (2012).
13. Hiesinger, H. *et al.* How old are young lunar craters? *J. Geophys. Res.* **117,** E00H10 (2012).
14. Gault, D. E. Saturation and equilibrium conditions for impact cratering on the lunar surface: Criteria and implications. *Radio Sci.* **5,** 273–291 (1970).
15. Lucey, P. G., Blewett, D. T., Taylor, G. J. & Hawke, B. R. Imaging of lunar surface maturity. *J. Geophys. Res.* **105,** 20377–20386 (2000).
16. Zanetti, M., Jolliff, B. L., van der Bogert, C. H. & Hiesinger, H. New determination of crater size-frequency distribution variation on continuous ejecta deposits: Results from Aristarchus crater. *Lunar Planet. Sci. Conf.* **44,** abstr. 1842 (2013).
17. Brett, R. Thicknesses of some lunar mare basalt flows and ejecta blankets based on chemical kinetic data. *Proc. Lunar Sci. Conf.* **6,** 1135–1141 (1975).
18. Schaber, G. G. Lava flows in Mare Imbrium: Geologic evaluation from Apollo orbital photography. *Proc. Lunar Sci. Conf.* **4,** 73–92 (1973).
19. Staid, M. I. *et al.* The spectral properties of Ina: New observations from the Moon Mineralogy Mapper. *Lunar Planet. Sci. Conf.* **42,** abstr. 2499 (2011).
20. Jolliff, B. L., Gillis, J. J., Haskin, L. A., Korotev, R. L. & Wieczorek, M. A. Major lunar crustal terranes: Surface expressions and crust-mantle origins. *J. Geophys. Res.* **105,** 4197–4216 (2000).
21. Warren, P. H. & Wasson, J. T. The origin of KREEP. *Rev. Geophys. Space Phys.* **17,** 73–88 (1979).
22. Head, J. W. & Wilson, L. Lunar mare volcanism: Stratigraphy, eruption conditions, and the evolution of secondary crusts. *Geochim. Cosmochim. Acta* **56,** 2155–2175 (1992).
23. Wieczorek, M. A. & Phillips, R. J. The 'Procellarum KREEP Terrane': Implications for mare volcanism and lunar evolution. *J. Geophys. Res.* **105,** 20417–20430 (2000).
24. Kneissl, T., van Gasselt, S. & Neukum, G. Map-projection-independent crater size-frequency determination in GIS environments-New software tool for ArcGIS. *Planet. Space Sci.* **59,** 1243–1254 (2011).
25. McEwen, A. S. & Bierhaus, E. B. The importance of secondary cratering to age constraints on planetary surfaces. *Annu. Rev. Earth Planet. Sci.* **34,** 535–567 (2006).
26. Schultz, P. H. & Spencer, J. Effects of substrate strength on crater statistics: Implications for surface ages and gravity scaling. *Proc. Lunar Sci. Conf.* **10,** 1081–1083 (1979).

27. van der Bogert, C. H. *et al.* Discrepancies between crater size-frequency distributions on ejecta and impact melt pools at lunar craters: An effect of differing target properties? *Lunar Planet. Sci. Conf.* **41,** abstr. 1533 (2010).
28. Dundas, C. M., Keszthelyi, L. P., Bray, V. J. & McEwen, A. S. The role of material properties in the cratering record of young platy-ridged lava on Mars. *Geophys. Res. Lett.* **37,** L12203 (2010).
29. Stöffler, D. & Ryder, G. Stratigraphy and isotope ages of lunar geologic units: Chronological standard for the inner solar system. *Space Sci. Rev.* **96,** 9–54 (2001).
30. Boyd, A. K., Robinson, M. S. & Sato, H. Lunar Reconnaissance Orbiter Wide Angle Camera photometry: An empirical solution. *Lunar Planet. Sci. Conf.* **43,** abstr. 2795 (2012).

Acknowledgements

This work was funded by the Lunar Reconnaissance Orbiter project and would not have been possible without the hard work of the Lunar Reconnaissance Orbiter Camera Science Operations Center team. Thank you to R. Wagner for help with figure preparation.

Author contributions

S.E.B. and M.S.R. conceived and designed the analyses. S.E.B. collected and analysed data; J.D.S. and S.E.B. both documented and characterized new IMPs. S.J.L. assisted in the interpretation of remote sensing data. C.H.v.d.B. and H.H. aided in the methodology and interpretation of CSFDs. S.E.B. wrote the manuscript with inputs from all authors.

Additional information

Supplementary information is available in the online version of the paper. Reprints and permissions information is available online at www.nature.com/reprints. Correspondence and requests for materials should be addressed to S.E.B.

Competing financial interests

The authors declare no competing financial interests.